

Analysis of a Turbulent Jet Mixing Flow by Using a PIV-PLIF Combined System

Hu, H.*¹, Saga, T.*², Kobayashi, T.*³. and Taniguchi, N.*²

- *1 Department of Mechanical Engineering, Michigan State University
A22, Research Complex Engineering Building, East Lansing, MI 48824, USA.
E-mail: huhui@egr.msu.edu
- *2 Institute of Industrial Science, University of Tokyo
4-6-1, Komaba, Meguro-ku, Tokyo 153-8505, Japan.
E-mail: saga@iis.u-tokyo.ac.jp
- *3 Japan Automobile Research Institute,
2530 Karima, Tsukuba, Ibaraki 305-0822, Japan.

Received 15 February 2003
Revised 20 August 2003

Abstract: In the present paper, the development of a high-resolution PIV-PLIF combined system for the simultaneous measurements of velocity and passive scalar concentration fields is described. The high-resolution PIV-PLIF combined system is used to perform the simultaneous whole-field measurements of velocity and concentration in the near field of a turbulent jet mixing flow. The characteristics of the mass transfer process and momentum transfer process in the near field of the jet mixing flows are discussed in the terms of ensemble-averaged velocity and concentration, turbulent intensity, concentration standard deviation and the correlation terms between the fluctuating velocities and concentration.

Keywords: PIV-PLIF combined system, Turbulent jet flow, Turbulent flux measurement

1. Introduction

It is highly desirable to get simultaneous information of a passive scalar and velocity field in many fluid flow investigations like mixing in combustion chambers or distributions of drugs in biomedical applications. It is also of fundamental importance to measure velocity and a scalar at the same time with high spatial and/or temporal resolution for the validation and development of models of turbulence and turbulent mixing. For example, in a turbulent jet mixing flow, the species concentration field is determined by molecular diffusion and transported by the turbulent flow field. When considering the Reynolds-averaged scalar conservation equation, the effects of turbulent transport appear in terms of the correlation between the concentration and velocity fluctuations, i.e. expressions such as $\overline{u'\xi'}$ and $\overline{v'\xi'}$. Experimental characterization of these correlation terms is needed for the development and validation of physical models. This requires the simultaneous measurements of the velocity and concentration fields.

There exists an extensive body of literature on the measurements of either velocity component or scalar quantitative (e.g. temperature, concentration) in many types of flows. However, studies

involving simultaneous velocity and scalar measurements in fluid flows are much less. One of the earliest was study of helium jet by Keagy and Weller (1949), in which the profiles of mean velocity was measured by using a Pitot probe and mean concentration using a sampling probe. A two-sensor hot-wire probe was developed by Way and Libby in 1970, which is capable of monitoring fluctuations of both one velocity component and concentration in a low-speed helium jet. Chavray and Tutu (1978) used a cold-wire sensor mounted on an X-wire probe to achieve simultaneous measurements of two fluctuating velocity components and temperature fluctuations in heated air jets. The investigations mentioned above provide examples of simultaneous measurements of velocity and a scalar quantity based on intrusive probes.

The advent of optical diagnostics such as Laser Doppler Velocimetry (LDV), Laser Induced Fluorescence (LIF) and Particle Scattering techniques have provided new opportunities for the non-intrusive simultaneous acquisition of multiple flow variables. A combination of LDV and LIF techniques was firstly used by Owen (1976) to do simultaneous measurements of velocity and concentration in a co-axial liquid jet. By using LDV/Mie scattering and LDV/Raman scattering techniques, Dibble and Schefer (1983) conducted simultaneous measurements of velocity, density and species concentration in a diffusions flame. Similar to the earlier work of Owen (1976), Lemoine et al. (1996) obtained simultaneous velocity and concentration data using LDV and LIF techniques in a liquid jet flow. All of these investigations, however, have incorporated single point measurements.

With the rapid development of modern optical techniques and digital image processing techniques, whole-field optical diagnostic techniques, such as Particle Imaging Velocity (PIV) and Planar Laser Induced Fluorescence (PLIF) techniques, are assuming ever-expanding roles in the diagnostic probing of fluid mechanics. The advances of PIV and PLIF techniques in recent years have lead them to be mature techniques for the whole-field measurements of velocity and concentration or/and temperature in an objective plane or even over a volume of an objective fluid flow. By combining the PIV and PLIF techniques, several studies have been conducted to achieve simultaneous measurements of instantaneous velocity and concentration distributions in turbulent flows (Law and Wang, 2000, Webster et al. 2001 and Cowen et al. 2001). In the present paper, the development of a high-resolution PIV-PLIF combined system will be described. An application of the high-resolution PIV-PLIF combined system to a turbulent jet mixing flow will be presented to study the mass transfer process and the momentum transfer process in the near field of the turbulent jet mixing flow. The characteristics of the mass transfer process and the momentum transfer process in the turbulent jet mixing flow will be discussed in terms of the distributions of the mean and turbulent fluctuation of velocity and concentration together with the correlation terms between the fluctuating velocities and concentration.

2. Experimental Setup and Techniques

Figure 1 shows the schematically experimental setup used in the present study. A test circular nozzle ($D=30\text{mm}$) was installed in the middle of a water tank ($600\text{mm}\times 600\text{mm}\times 1000\text{mm}$). Fluorescent dye (Rhodamine B, concentration is about $0.6\times 10^{-6}\text{M}$) for PLIF and hollow glass particles ($8\sim 12\mu\text{m}$ in diameters) for PIV measurement were premixed with water in a jet supply tank, and the jet flow was supplied by a pump. The flow rate of the jet flow, used to calculate the representative velocity and Reynolds numbers, was measured by using a flow meter. A cylindrical plenum chamber filled with

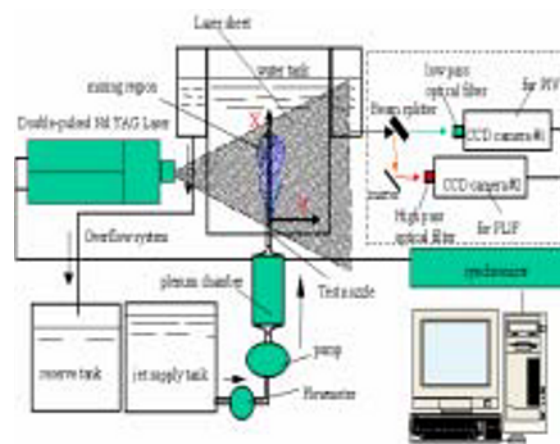


Fig. 1. Experimental system setup.

honeycomb and mesh structures was installed at the upstream of the test nozzle to insure the jet flow to be fully developed. The turbulent level in the center of the jet flow was about 3% at the exit of test nozzle. An overflow system was designed to keep the water level in the test tank to be constant during the experiment. In the present study, the investigation region is the near field of the jet flow ($Y/D < 5.0$). The distance between the exit of the test nozzle and the water free surface in the test tank is about $30D$. Therefore, the effect of the water free surface on the vortical and turbulent structures in the near field of the jet flow is negligible, and the jet flow exhausted from the test nozzle is considered to be a free jet. During the experiment, the core jet velocities (U_0) at the exit of the test nozzle was set to be about 0.2m/s . The Reynolds numbers of the jet flow, based on the nozzle exit diameter and the core jet velocity is about 6,000.

Pulsed laser sheets (thickness is about 1.0mm) generated by a double-pulsed Nd:YAG Laser system (Quantel Inc.) were used to illuminate the measurement region. The frequency of the double-pulsed illumination is 10Hz . The duration of the pulsed illumination is 4ns , and power is 200mJ/pulse . The time interval between the two pulses is adjustable, which is 4ms for the present study.

Figure 2 shows a simultaneous image recording system, which is set up by using optics and two high-resolution CCD cameras (TSI PIVCAM10-30, 1K by 1K resolution). Since the emission peak of Rhodamine B is about 590nm , and the wavelength of the illuminating laser light scattered by the PIV tracer particles is 532nm . Two kinds of optical filters were used to separate the LIF lights from the scattered laser lights, and then recorded them separately to obtain PLIF and PIV image simultaneously. A bandpass optical filter ($532 \pm 5\text{nm}$) was installed at the head of the camera #1, only the scattered laser light is transmissible to form PIV image on the CCD sensor of the camera #1, and LIF light is blocked out. A high pass filter ($>580\text{nm}$ pass) was installed in the head of the camera #2 to filter out the scattered laser light (wavelength 532nm). The LIF light (peak at 590nm) pass through the optical filter to generate LIF image on the CCD sensor of the camera #2.

Figure 3 shows an example of the typical PLIF and PIV original images captured by the camera #1 and #2 simultaneously. It can be seen that the scattered laser light and LIF light were separated successfully by using the simultaneous image recording system described above.



Fig. 2. The photograph of the PIV-PLIF simultaneous image recording system.



(a) PIV image from camera #1



(b) PLIF image from camera #2

Fig. 3. Typical instantaneous images captured by the simultaneous image recording system.

3. Image Processing

3.1 PIV Image Processing

Most common used methods for PIV image processing can be categorized into two groups: particle tracking methods and spatial correlation analysis methods (including auto-correlation methods and cross-correlation methods). Particle tracking methods are based on the tracking of individual particles with the time sequence, and vectors are obtained at random points in space. Rather than tracking individual particles, spatial correlation analysis methods are used to obtain the average displacement of the ensemble particles. The recorded PIV images were divided into many smaller sub-regions (which are called interrogation windows). Each interrogation window contains several particle images. Analysis of the displacement of images in each interrogation window by means of spatial correlation operation (either cross-correlation or auto-correlation) leads to an estimated average displacement of particles included in the interrogation window. This approach is valid for the case in which many particle images were included in per interrogation window, referred to as the high image density limit (Adrian, 1991).

By using spatial correlation analysis methods, the obtained velocity vector is actually the spatially averaged velocity of the particles included in each interrogation window. The spatial resolution of the final PIV results is directly related to the size of the interrogation windows. In order to improve the spatial resolution of the PIV results, the size of the interrogation window should be reduced as small as possible. However, according to the study of Keane and Adrian (1990), at less ten-tracer particle images per interrogation window should be satisfied in order to resolve the local particle displacement accurately by using the conventional correlation analysis based image-processing algorithms. Hu et al. (1998) also suggested that the optimum particle number in an interrogation window be about 10-20 for conventional cross-correlation method. These indicate that interrogation window size should be big enough to contain sufficient number of particle images to insure a high probability of uniqueness of the solution by using conventional correlation analysis methods for PIV image processing.

It was found that if a prior information of the local displacement is known, statistically meaningful results could be obtained even by using a smaller interrogation window. Based on this ideal, an improved spatial correlation analysis method, named as Hierarchical Recursive PIV (HR-PIV) method was developed by the authors (Hu et al. 2000), which is similar to the discrete window offset method suggested by Westerweel et al. (1997). The HR-PIV method is actual a hierarchical recursive process of conventional spatial correlation method. The recursive operation started with a large interrogation window size and search distance, which is as the same as conventional correlation analysis methods. By using the results of former iteration step as the approximate offset values in the next iteration step, the interrogation window size and search distance were reduced hierarchically. The HR-PIV method was used in the present study to conduct PIV image processing. Conventional correlation analysis methods always need to use 64 by 64 pixel or 32 by 32 pixel interrogation windows, the HR-PIV method used in the present study can reduce the final interrogation window up to 8 by 8 pixel with spurious vectors being less than 2%.

3.2 PLIF Image Processing

Following the work of Coppeta and Rogers (1998), the intensity of the laser induced fluorescence light at an arbitrary point (x_0, y_0) along the excitation beam for unsaturated excitation can be expressed as:

$$H_f(x_0, y_0) = I(x_0, y_0)A\Phi \varepsilon L \xi(x_0, y_0) \quad (1)$$

where $H(x_0, y_0)$ is the detected fluorescence intensity at the measurement point (x_0, y_0) , A is the

fraction of the fluorescence light collected by camera. Φ is the quantum efficiency, L is the length of the sampling volume along the path of excitation beam, ε is the molar absorptivity, and $\xi(x_0, y_0)$ is the molar concentration of the fluorescent dye. $I(x_0, y_0)$ is the intensity of excitation light beam at the measurement point (x_0, y_0) .

It should be noted that the intensity of the excitation light $I(x_0, y_0)$ is the function of the position and the concentration distribution of the fluorescent dye along the excitation beam before reaching the measurement point (x_0, y_0) . The concentration distribution of the fluorescent dye may attenuate the intensity of the excitation beam. The attenuation effect will be increasing with the increasing of the concentration of the fluorescent dye (Hu et al. 1999). In order to minimize the attenuation effect, a low fluorescent-dye-concentration solution ($\xi_0 = 0.6 \times 10^{-6}$ M) was used for the present study.

From the equation (1), it can be seen that the intensity of induced fluorescent light detected by the image recording camera will be changed linearly with the concentration of the fluorescent dye for the constant properties of carrier flow (temperature, oxygen content, pH value etc.) when the attenuation effect is negligible. For experimental conditions used in the present study, a calibration procedure has been conducted to confirm such linear relationship, and the calibration profiles are shown in Fig. 4.

In order to obtain whole-field concentration distribution, a calibration procedure to account for the non-uniformity of the laser illumination was conducted in the present study. For fixed optical setting, the linear relationship between the molar concentration of the fluorescent dye $\xi(x, y)$ in the fluid flow and the digital signal level $i_d(x, y)$ can be expressed by the following equation:

$$i_d(x, y) - i_{background}(x, y) = k(x, y)\xi(x, y) \quad (2)$$

$k(x, y)$ in the above equation included variations in laser energy over the illuminating laser sheet. $i_{background}(x, y)$ is the background noise in the digital LIF image.

The background noise $i_{background}(x, y)$ is determined firstly by taking 50 images of the objective field without fluorescent dye but with scattering of PIV particles and illuminating of laser sheet. Then, the mean digital signal level $i_{d\xi_0}(x, y)$ with known uniform concentration ($\xi_0 = 0.6 \times 10^{-6}$ M) in the measurement region is determined by taking 50 images.

According to the equation (2), the following equation can be obtained

$$i_{d\xi_0}(x, y) - i_{background}(x, y) = k(x, y)\xi_0(x, y) \quad (3)$$

Therefore, the normalized concentration distribution in the objective fluid flow can be calculated by using following equation:

$$c(x, y) = \frac{\xi(x, y)}{\xi_0(x, y)} = \frac{k(x, y)\xi(x, y)}{k(x, y)\xi_0(x, y)} = \frac{i_d(x, y) - i_{background}(x, y)}{i_{d\xi_0}(x, y) - i_{background}(x, y)} \quad (4)$$

Since the final interrogation window size is 8 by 8 pixel for the present study, the concentration data were also averaged over 8 by 8 subwindows during the PLIF image processing. Once the

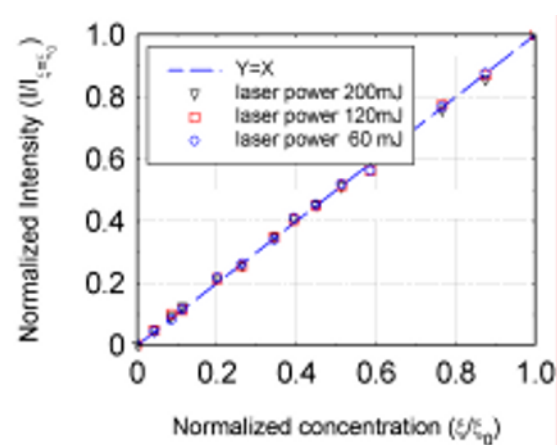


Fig. 4. Calibration profiles for the concentration measurement.

simultaneous velocity and concentration data were obtained, it is relatively straightforward to calculate various ensemble-averaged velocity (U, V), turbulent fluctuations ($\sqrt{\overline{u'u'}}, \sqrt{\overline{v'v'}}$), mean concentration (C), concentration standard deviation ($\sqrt{\overline{c'c'}}$) and the turbulent flux terms ($\overline{u'c'}, \overline{v'c'}$) which are the correlation terms between the velocity and concentration.

For the measurement result given in the present study, the error level of the PIV measurement result is estimated to be about 2.0%, and the error level for the PLIF concentration measurement is estimated to be less than 3.0%.

4. Experimental Results and Discussions

Figure 5 shows a typical pair of instantaneous PIV and PLIF measurement results of the PIV-PLIF combined system. Since the final interrogation window size in the present study is 8 pixels by 8 pixels (0.8×0.8mm in space) for PIV image processing, about 50,000 vectors were obtained for each instantaneous PIV frame. The velocity vectors shown in Fig. 5(a) display only 25% of the total PIV velocity vectors. Fig. 5(b) shows the instantaneous concentration distribution, which is the simultaneous measurement result of the instantaneous PIV results shown in Fig. 5(a). The contour levels given in the figure represent Rhodamine B molar concentration levels normalized by the jet source concentration ($\xi_0 = 0.6 \times 10^{-6} M$). It is well known that the shear layers originating from the trailing edge of the test nozzle are unstable via Kelvin-Helmholtz instability. The instability grows downstream and rolled up into coherent vortex rings. The vortex ring structures merge as they move downstream, and then break down into many small vortex structures. The transition of the jet flow into turbulence occurs when the large vortex rings break down into small-scale vortices. All these processes can be seen clearly and quantitatively from the PIV-PLIF simultaneous measurement results shown in Fig. 5.

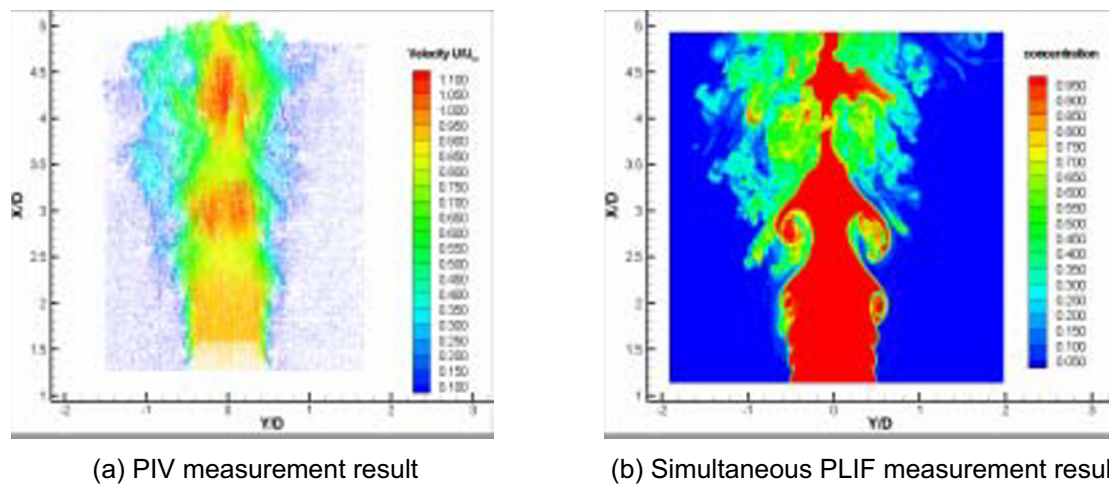


Fig. 5. Typical instantaneous measurement results of the PIV-PLIF combined system.

In the present study, 250 frames of the PIV and PLIF image pairs captured simultaneously at the frame rate of 10Hz were used to calculate the ensemble-averaged values. The ensemble-averaged values were normalized with the core jet velocity $U_{in} = 0.2$ m/s and jet source concentration ($\xi_0 = 0.6 \times 10^{-6} M$). Figure 6 shows the distributions of various ensemble-averaged terms, which include ensemble-averaged velocity ($U/U_{in}, V/U_{in}$), ensemble-averaged concentration (ξ/ξ_0), turbulent intensity ($\frac{\sqrt{\overline{u'u'} + \overline{v'v'}}}{U_{in}}$), concentration standard deviation ($\frac{\sqrt{\overline{c'c'}}}{\xi_0}$) and the axial and radial

turbulent flux terms $(\frac{\overline{u'\xi'}}{U_{in}\xi_0}, \frac{\overline{v'c'}}{U_{in}\xi_0})$.

It is well known that momentum transfer process in a fluid flow can be represented from the velocity distributions, and mass transfer process can be revealed directly from the concentration fields. The characteristics of the momentum transfer process and the mass transfer process in the near field of the turbulent jet mixing flow can be compared based on the simultaneous velocity and concentration measurement results obtained by using the high-resolution PIV-PLIF combined system.

From the distributions of the ensemble-averaged velocity (Fig. 6(a)) and ensemble-averaged concentration (Fig. 6(b)), it can be seen that there exists a region with constant velocity or constant concentration in the center of the jet flow, which is called potential core region. The comparison between the ensemble-averaged velocity distribution and ensemble-averaged concentration distribution shows that the length of the velocity potential core region is longer than that of the concentration potential core region. It may be because the Schmidt number of Rhodamine B in water is much bigger than 1, therefore, the mass transfer process conducts more rapidly than the momentum transfer process in the near region of the jet mixing flow, which results in the faster decay of the potential core region in the concentration field than that in the velocity field.

In the potential core regions, the turbulent intensity (Fig. 6(c)) and the concentration standard deviation are (Fig. 6(d)) very low. High turbulent intensity and high concentration fluctuation regions exist in the mixing layers between the core jet flow and ambient flow. The high concentration standard deviation regions were found to concentrate more upstream compared with those in the turbulent intensity distribution. In the mixing layers, the Reynolds stress level was also found to be quite high as it is expected (Fig. 6(e)). The turbulent flux vectors $(\frac{\overline{u'\xi'}}{U_{in}\xi_0}, \frac{\overline{v'c'}}{U_{in}\xi_0})$ are shown in Fig. 6(f),

which indicates how the LIF dye molecules are transported from the core jet flow to ambient flow via the mixing between the two streams. The turbulent flux vector plot reveals the mass transfer process in the near field of the turbulent jet mixing flow very clearly and quantitatively.

Figure 7 shows the profiles of the ensemble-averaged flow variables in three typical downstream locations of the turbulent jet mixing flow. The measurement results of Lemoine et al. (1996) by using single point measurement techniques (LDV and LIF) at 4D downstream of a circular jet flow with the same Reynolds level as the present study are also given in the figures. It can be seen that the present PIV-PLIF simultaneous measurement results agree with the measurement results of Lemoine et al. (1996) reasonably well. The comparison of the ensemble-averaged velocity profile with the ensemble-averaged concentration profiles shows a faster “round-up” of the ensemble-averaged concentration profiles as the downstream distance increases, which is consistent with the result that the mass transfer process conducts more rapidly than the momentum transfer process as mentioned above. The regions with high fluctuation values in the turbulent intensity profiles (Fig. 7(c)) and the concentration standard deviation profiles (Fig. 7(d)) are corresponded to the mixing layers between the core jet flow and ambient flow. The comparison of the two groups of fluctuation profiles shows that the width of the mixing layers revealed in the concentration standard deviation profiles are much wider, which also indicates the faster growth of the mass transfer process than that of the momentum process. Fig. 7(e) and Fig. 7(f) give the axial turbulent flux $\frac{\overline{u'\xi'}}{U_{in}\xi_0}$ and radial turbulent flux $\frac{\overline{v'c'}}{U_{in}\xi_0}$ profiles. They were found to be almost bell-shaped profiles.

Although the ensemble-averaged axial velocity component is much bigger than the radial velocity component in the near field of the turbulent jet flow, the axial turbulent flux $\frac{\overline{u'\xi'}}{U_{in}\xi_0}$ and radial

turbulent flux $\frac{\overline{v'c'}}{U_{in}\xi_0}$ were found to be almost at the same order from the measurement results.

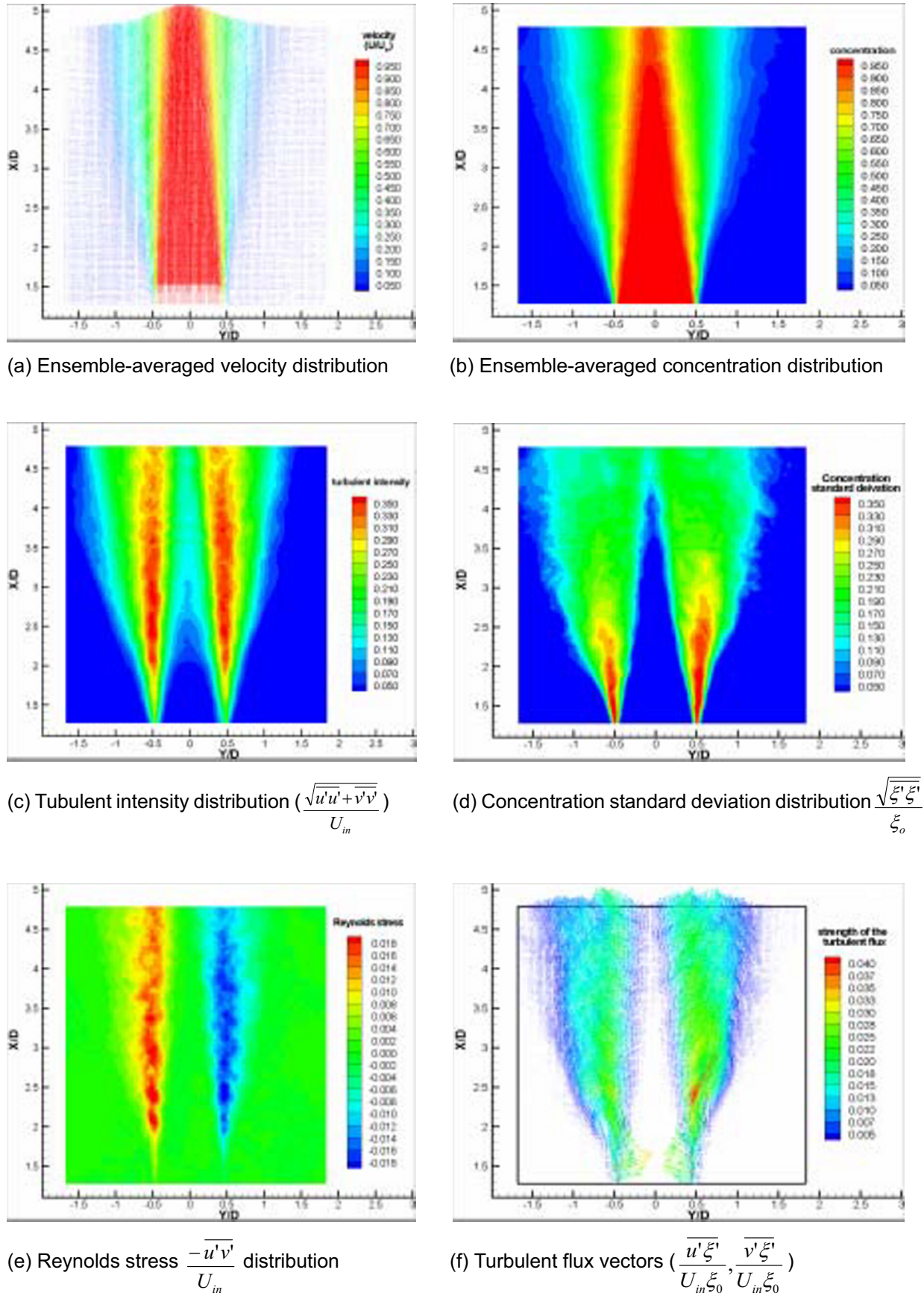


Fig. 6. Ensemble-averaged measurement results.

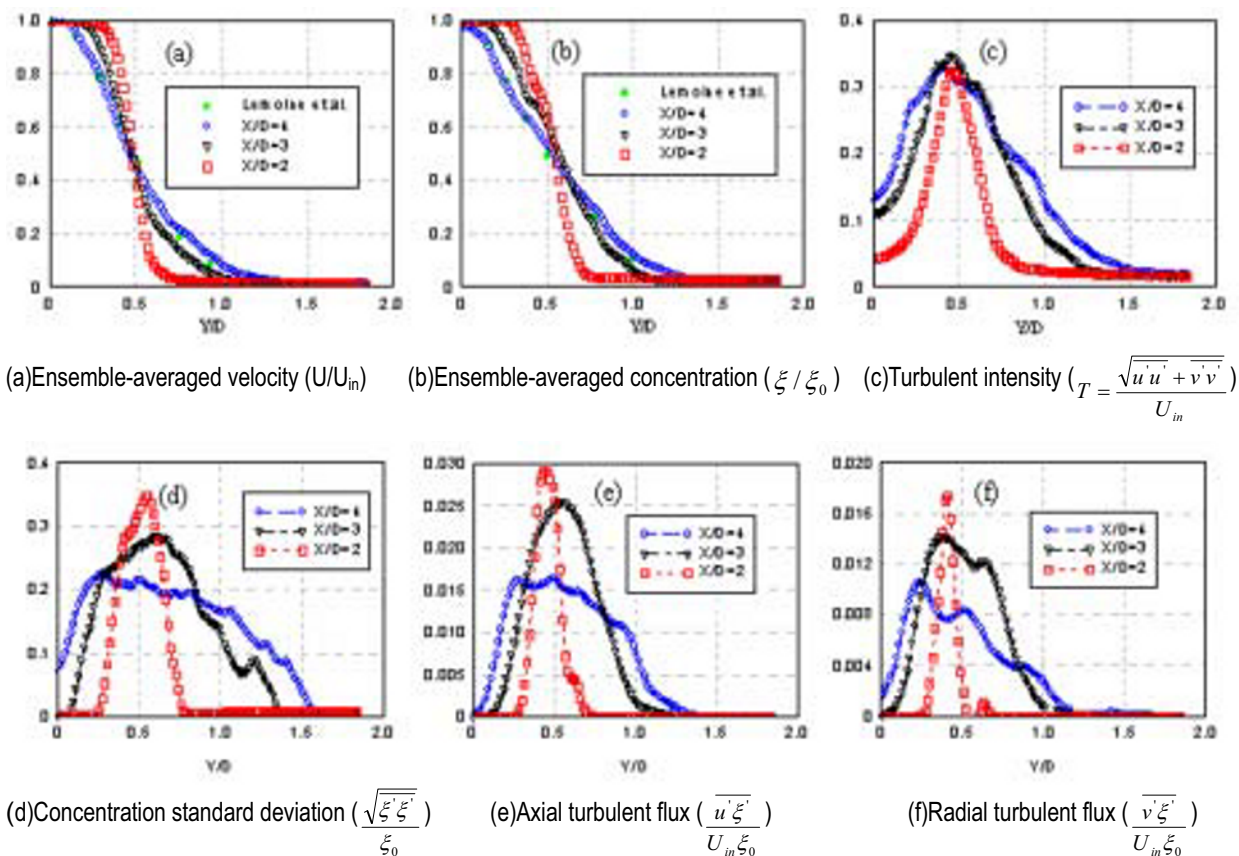


Fig. 7. The profiles of the ensemble-averaged results.

4. Conclusion

The development of a high-resolution PIV-PLIF combined system, which can achieve simultaneous measurements of the velocity and concentration distributions in fluid flows, was described in the present paper. The high-resolution PIV-PLIF combined system was used to study the mass transfer process and momentum transfer process in the near field of a turbulent jet flow. The characteristics of the mass transfer process and momentum transfer process in the turbulent jet flow were compared in the terms of ensemble-averaged velocity and concentration, turbulent intensity, concentration standard deviation and the correlation terms between the fluctuating velocities and concentration. It was found that the mass transfer process conducted more rapidly in the near field of the turbulent jet mixing flow compared with the momentum transfer process.

References

- Adrian R. J., Particle-Imaging Techniques for Experimental Fluid Mechanics, *Ann. Rev. Fluid Mech.*, 23 (1991), 261.
- Chevary, R. and Tutu, N. K., Intermittence and Preferential Transport of Heat in a Round Jet. *Journal of Fluid Mechanics*, (1978), 133.
- Coppeta J. and Rogers C., Dual Emission Laser Induced Fluorescence for Direct Planar Scalar Behavior Measurements, *Experiments in Fluids*, 25-1 (1998), 1-15.
- Cowen, E. A., Chang, K. -A. and Liao, Q., A Single Camera Coupled PTV-LIF Technique, *Experiments in Fluids*, 31 (2001), 63-73.
- Dibble, R. W. and Schefer, R. W., Simultaneous Measurements of Velocity and Scalars in a Turbulent Non-promixed flame by Combined Laser Doppler Velocimetry and Laser Raman Scattering, *Proceedings of 4th Turbulent Shear Flows Karlsruhe, Germany*, (1983), 12-14.
- Hu, H., Saga, T., Kobayashi, T., Okamoto, K. and Taniguchi, N., Evaluation of the Cross Correlation Method by Using PIV Standard Images *Journal of Visualization*, 1-1 (1998), 87-94.
- Hu, H., Kobayashi, T., Wu, S. and Shen, G., Research on the Vortical and Turbulent Structure Changes of Jet Flow by Mechanical Tabs, *Journal of Mechanical Engineering Science*, 213 (1999), 321-329.

- Hu, H., Saga, T., Kobayashi, T., Taniguchi, N. and Segawa, S., Improve the Spatial Resolution of PIV Results by Using Hierarchical Recursive Operation, Proc. of 9th International Symposium on Flow Visualization, Edinburgh, Scotland, UK, Aug. (2000), 22-25.
- Keagy, W. R. and Weller, A. E., A Study of Freely Expanding Inhomogeneous Jets, Proc. Heat Transfer, Fluid Mechanics Inst., 1-3 (1949), 89-98.
- Keane, R. D. and Adrain, R. J., Optimization of Particle Image Velocimetry, Measurement Science and Technology, 2 (1990), 1202-1215.
- Law, A. W. -K. and Wang, H., Measurement of Mixing Processes with Combined Digital Particle Image Velocimetry and Planar Laser Induced Fluorescence, Experimental Thermal and Fluid Science 22 (2000), 213-229.
- Lemoine, F., Wolff, M. and Lebouche, M., Simultaneous Concentration and Velocity Measurements Using Combined Laser-Induced Fluorescence and Laser Doppler Velocimetry: Application to Turbulent Transport, Experiments in Fluids, 20 (1996), 341-327.
- Owen, F. K., Simultaneous Laser Measurements of Instantaneous Velocity and Concentration in Turbulent Mixing Flows, Proceeding of AGARD Conference On Applications of Non-Intrusive Instrumentation in Fluid Flow Research AGARD-CP-193 (1976).
- Way, J. and Libby, P. A., Hot-wire Probes for Measuring Velocity and Concentration in Helium and Air Mixture AIAA Journal, 8 (1970), 976-978.
- Webster, D. R., Roberts, P. J. W. and Ra'ad, L., Simultaneous DPTV/LIF Measurements of a Turbulent Jet, Experiments in Fluids 30 (2001), 65-72.
- Westerweel, J., Dabiri, D. and Gharib, M., The Effect of a Discrete Window Offset on the Accuracy of Cross-Correlation Analysis of Digital PIV Recordings Experiments in Fluids, 23 (1997), 20-8.

Author Profiles



Hui HU: He is working as a Research Associate and Course Instructor at the Department of Mechanical Engineering, Michigan State University. He received his Ph.D degrees from the University of Tokyo (Mechanical Engineering) in 2001 and Beijing University of Aeronautics and Astronautics (Aerospace Engineering) in 1996. His research interests include development of advanced optical diagnostic techniques for fluid flow and heat transfer, and fundamental studies of complex fluid flow and heat transfer phenomena.



Tetsuo Saga: He graduated from Japan University in 1966 and he is a Research Associate in the Institute of Industrial Science University of Tokyo. His main research field is mechanical engineering. His research interests are flow visualization and its image analysis, prediction and control of flow induced aero-noise and multiphase flow dynamics. Recently, he has interesting in micro flow and bio flow analysis using by micro PIV.



Toshio Kobayashi: He received his Ph.D. in Mechanical Engineering Department, the University of Tokyo in 1970. After completion his Ph.D. program, he has been faculty member of the Institute of Industrial Science (IIS) University of Tokyo, and currently is Project leader of "Frontier Simulation Software for Industrial Science" IIS University of Tokyo and Director of Japan Automobile Research Institute (JARI). His research interests are numerical analysis of turbulence, especially Large Eddy Simulation, and Particle Image Velocimetry. He serves as the President of Visualization Society of Japan (VSJ), Executive Vice President of Automotive Engineer of Japan (JSAE) and President of the Japan Society of Mechanical Engineers (JSME).



Nobuyuki Taniguchi: He received his Ph.D. in Marine Engineering Department, the University of Tokyo in 1989. After completion his Ph.D. program, he has been faculty member of the Institute of Industrial Science (IIS) University of Tokyo, and since 2000 is an associate professor at Intelligent Technology Center. His research interests are computational methods for numerical modeling and measurement system of fluid flows, which applied to complex turbulence such as combustion flows and multiphase phenomena.